The EMBO Journal Vol.17 No.22 pp.6678–6688, 1998

Control of Swe1p degradation by the morphogenesis checkpoint

Rey A.L.Sia, Elaine S.G.Bardes and Daniel J.Lew[1]

Department of Pharmacology and Cancer Biology, Duke University Medical Center, Durham, NC 27710, USA

[1]Corresponding author
e-mail: daniel.lew@duke.edu

In the budding yeast *Saccharomyces cerevisiae*, a cell cycle checkpoint coordinates mitosis with bud formation. Perturbations that transiently depolarize the actin cytoskeleton cause delays in bud formation, and a 'morphogenesis checkpoint' detects the actin perturbation and imposes a G_2 delay through inhibition of the cyclin-dependent kinase, Cdc28p. The tyrosine kinase Swe1p, homologous to wee1 in fission yeast, is required for the checkpoint-mediated G_2 delay. In this report, we show that Swe1p stability is regulated both during the normal cell cycle and in response to the checkpoint. Swe1p is stable during G_1 and accumulates to a peak at the end of S phase or in early G_2, when it becomes unstable and is degraded rapidly. Destabilization of Swe1p in G_2 and M phase depends on the activity of Cdc28p in complexes with B-type cyclins. Several different perturbations of actin organization all prevent Swe1p degradation, leading to the persistence or further accumulation of Swe1p, and cell cycle delay in G_2.
Keywords: budding yeast/cell cycle/checkpoint/degradation/Swe1p

Introduction

Entry into mitosis is triggered by activation of the cyclin-dependent kinase cdc2 by mitotic B-type cyclins (reviewed by Nurse, 1990; Morgan, 1995). An important mechanism governing the activity of the cdc2–cyclin complex is the inhibitory phosphorylation of cdc2 at a conserved tyrosine residue, catalyzed by wee1-related kinases (reviewed by Dunphy, 1994). Tyrosine dephosphorylation of cdc2 by the cdc25 phosphatase is the key event that triggers entry into mitosis during the cell cycle of the fission yeast *Schizosaccharomyces pombe* and probably many other cells (reviewed by Dunphy, 1994). However, tyrosine phosphorylation of Cdc28p (the cdc2 homolog) does not participate in mitotic control of the unperturbed cell cycle in the budding yeast *Saccharomyces cerevisiae* (Amon *et al*., 1992; Sorger and Murray, 1992).

Coordination of cell cycle events during cell proliferation is attained, in part, through surveillance pathways called checkpoint controls (reviewed by Hartwell and Weinert, 1989; Murray, 1992; Lew *et al*., 1997). Checkpoint controls monitor key processes during the cell cycle, and act to delay cell cycle progression if those processes are defective. For instance, entry into mitosis is delayed in cells containing damaged or incompletely replicated DNA (reviewed by Elledge, 1996). It is now well established that cdc2 tyrosine phosphorylation is required for the arrest of mitosis triggered by both the DNA damage checkpoint and the DNA replication checkpoint in *S.pombe* (Rhind *et al*., 1997; Rhind and Russell, 1998 and references therein), and this is true, at least in part, for many other cells (though not for *S.cerevisiae*; reviewed by Lew and Kornbluth, 1996; see also Blasina *et al*., 1997). However, only recently have the links between these checkpoints and the enzymes controlling cdc2 tyrosine phosphorylation begun to emerge (Furnari *et al*., 1997; O'Connell *et al*., 1997; Peng *et al*., 1997; Sanchez *et al*., 1997; Boddy *et al*., 1998), and our understanding of how these checkpoints cause cell cycle arrest is far from complete.

In *S.cerevisiae*, a morphogenesis checkpoint delays nuclear division when the actin cytoskeleton is perturbed (Lew and Reed, 1995; McMillan *et al*., 1998). Various environmental stresses cause a temporary disruption of cytoskeletal polarity, leading to a delay of bud formation. If mitosis were to continue unchecked, cells lacking large enough buds would become binucleate; the checkpoint prevents this fate by providing time for recovery of actin polarity and completion of bud formation prior to mitosis. During the checkpoint-induced delay, cell cycle progression is halted by inhibitory phosphorylation of Cdc28p (the *S.cerevisiae* homolog of cdc2) at Tyr19 (Lew and Reed, 1995). Thus, the same biochemical regulatory pathway has been utilized to arrest the cell cycle in response to different checkpoint controls in different organisms.

Phosphorylation of Cdc28p at Tyr19 is catalyzed by the protein kinase Swe1p (the *S.cerevisiae* homolog of wee1), while dephosphorylation is catalyzed by Mih1p (the *S.cerevisiae* homolog of cdc25) (Russell *et al*., 1989; Booher *et al*., 1993). Cells lacking Swe1p exhibit cell cycle kinetics identical to those of wild-type cells, but are unable to delay mitosis in response to actin-perturbing conditions (Sia *et al*., 1996; McMillan *et al*., 1998). These observations suggested that the morphogenesis checkpoint might increase Swe1p abundance or activity. In this report, we investigate the behavior of Swe1p during cell cycle progression and during checkpoint arrest following perturbation of morphogenesis.

Results

Swe1p accumulates during a checkpoint response

To examine the behavior of Swe1p, we first generated an epitope-tagged version of Swe1p, Swe1p-myc, which was expressed from an integrated single copy at the *SWE1* genomic locus (see Materials and methods; Figure 1A). To assess whether the tag affected Swe1p function, we performed pheromone arrest–release synchrony experi-

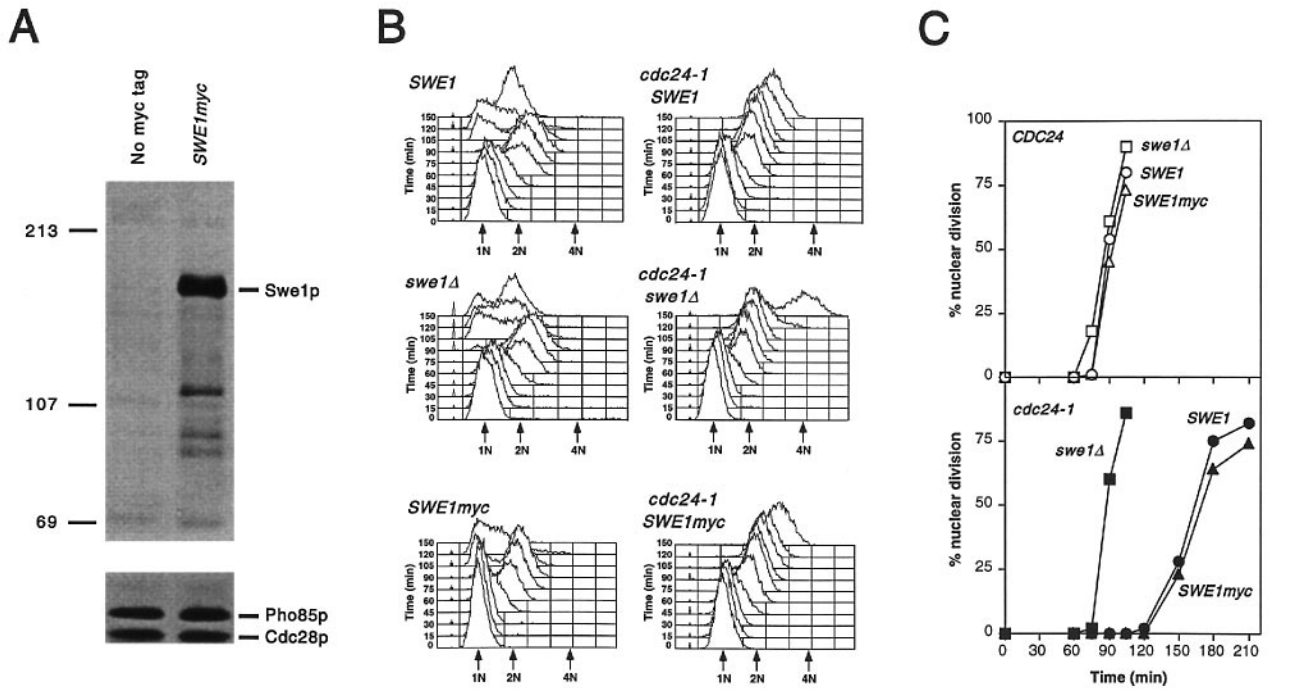

Fig. 1. Characterization of Swe1p-myc. (**A**) Immunoblot analysis of cells expressing or lacking the *SWE1myc* construct: Swe1p-myc migrates as a fuzzy band at ~180 kDa. (**B**) Flow-cytometric analysis of synchronized cell populations with the indicated genotypes released from pheromone arrest ($t = 0$). (**C**) Quantitation of cumulative percentage nuclear division for the same samples as in (B). The Swe1p-myc fully complements the G_2 delay in *cdc24-1* mutants lacking Swe1p. The strains used were DLY1 (*SWE1*), DLY1028 (*swe1*Δ), RSY311 (*SWE1myc*), DLY657 (*cdc24-1 SWE1*), DLY690 (*cdc24-1 swe1*Δ) and RSY258 (*cdc24-1 SWE1myc*).

ments to compare cell cycle progression in cells containing tagged versus untagged Swe1p. As demonstrated previously (Booher *et al*., 1993; Sia *et al*., 1996), Swe1p had no effect on the timing of DNA replication (45–60 min; Figure 1B) or nuclear division (75–105 min; Figure 1C) in the unperturbed cell cycle. The tagged Swe1p-myc did not alter cell cycle kinetics in these cells (Figure 1B and C). Temperature-sensitive *cdc24-1* mutants are unable to polarize actin (Adams and Pringle, 1984), and these mutants exhibited a prolonged G_2 phase between DNA replication (45–60 min; Figure 1B) and nuclear division (150–180 min; Figure 1C). *cdc24-1* mutants lacking Swe1p did not undergo this G_2 delay, but progressed through nuclear division (75–105 min; Figure 1C) and a subsequent round of DNA replication (150 min; Figure 1B). The tagged Swe1p-myc was fully capable of restoring the G_2 delay in *cdc24-1* cells (Figure 1B and C). This experiment demonstrates that the tagged *SWE1-myc* complements the *swe1*Δ phenotype and therefore encodes a fully functional protein.

We next examined the behavior of Swe1p-myc during the unperturbed cell cycle and during a checkpoint response (Figure 2). We and others have reported previously that *SWE1* mRNA accumulation is periodic during the cell cycle, with a peak in late G_1 (Lim *et al*., 1996; Ma *et al*., 1996; Sia *et al*., 1996). Swe1p-myc protein accumulation was also periodic, but offset from the transcript abundance, peaking during S/G_2 and declining prior to and during nuclear division (McMillan *et al*., 1998 and Figure 2A; Swe1p-myc protein declined from peak levels to very low levels within 30 min). This demonstrates that Swe1p is an unstable protein, at least in the later part (G_2/M phase) of the unperturbed cell cycle.

In addition, Swe1p-myc migration during SDS–PAGE became retarded as cells progressed through the cell cycle (Figure 2). We show below that this is due to phosphorylation of Swe1p-myc.

To assess the behavior of Swe1p upon triggering of the morphogenesis checkpoint, we perturbed actin organization in three different ways: by applying an osmotic shock (Figure 2B), by depolarizing actin using the temperature-sensitive *cdc24-1* mutant (Figure 2C) and by constitutively impairing actin organization using a *tpm1* mutant (Figure 2D). *TPM1* encodes the major tropomyosin in yeast (Liu and Bretscher, 1989). These perturbations have different effects: osmotic shock causes a transient depolarization of actin followed by complete recovery (Chowdhury *et al*., 1992); *cdc24-1* (at the restrictive temperature) completely blocks actin polarization and bud formation (Sloat *et al*., 1981; Adams and Pringle, 1984); and *tpm1* constitutively impairs actin organization but permits bud formation and proliferation at a reduced rate (Liu and Bretscher, 1992). In all cases, Swe1p-myc accumulated to higher levels than normal and/or persisted for longer than normal under checkpoint-inducing conditions (Figure 2B–D).

Swe1p is stabilized during a checkpoint response

What is the basis for the persistence of Swe1p in cells responding to the checkpoint? We have shown that *SWE1* transcription is elevated in *cdc24-1* cells, and this undoubtedly contributes to the elevated Swe1p levels in these cells (Sia *et al*., 1996). However, cells were still able to regulate the length of the G_2 interval in response to the checkpoint when *SWE1* transcription was rendered constitutive (Sia *et al*., 1996), suggesting that other Swe1p regulatory pathways must exist. To test whether regulation

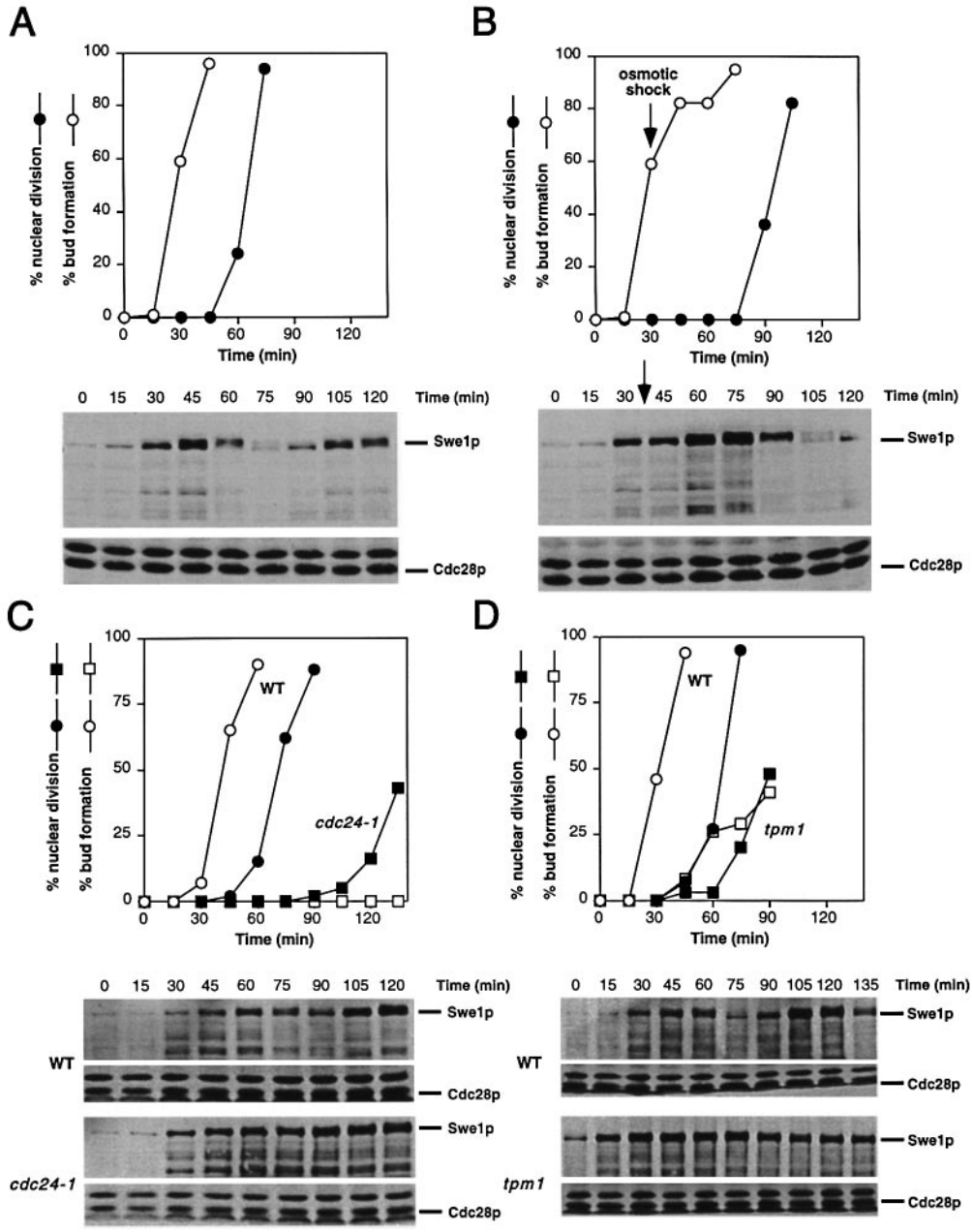

Fig. 2. Swe1p accumulates during a morphogenesis checkpoint response. (**A**) Pheromone arrest–release synchrony of wild-type cells (RSY206) in YEPD at 30°C. The cumulative percentage of cells that initiated bud formation or underwent chromosome separation is plotted for the same samples shown in the immunoblot. (**B**) Cells from the same culture used in (A) were exposed to 0.4 M NaCl at 30 min following release from pheromone arrest (arrow). This led to the continued accumulation of Swe1p for an additional 30 min, and a concomitant 30 min delay of anaphase. (**C**) Wild-type (RSY311) and *cdc24-1* (RSY258) cells were grown at 23°C, arrested in G_1 with pheromone, and released from the arrest at 37°C to prevent actin polarization in the *cdc24-1* cells. Swe1p levels remained high in the *cdc24-1* cells, and these cells exhibited a pronounced G_2 delay. (**D**) Pheromone arrest–release synchrony of wild-type cells (RSY311) and *tpm1* (RSY336) cells at 30°C. Swe1p levels remained high for some time in the *tpm1* cells, and these cells exhibited a G_2 delay.

of Swe1p degradation might play a role, we performed pulse–chase experiments to monitor Swe1p-myc stability directly under unperturbed or checkpoint-inducing conditions (Figure 3). For these experiments, strains containing a copy of *SWE1-myc* under the control of the regulatable *GAL1* promoter were grown in sucrose-containing media (non-inducing for the *GAL1* promoter), pulse-labeled for 10 min in galactose-containing media (inducing for the *GAL1* promoter) and chased in dextrose-containing media (repressing for the *GAL1* promoter; see Materials and methods for details). This set of experiments revealed that Swe1p-myc was stabilized transiently following osmotic shock (Figure 3A), and that it was stable for several hours in *cdc24-1* and *tpm1* mutant cells (Figure 3B). These data show that Swe1p is stable (>4 h half-life) in cells that have triggered the checkpoint.

Swe1p degradation is cell-cycle regulated

Two additional and unexpected findings emerged from these experiments. First, Swe1p-myc degradation did not appear to follow straightforward first-order kinetics in wild-type unperturbed cells (Figure 3, note the slower

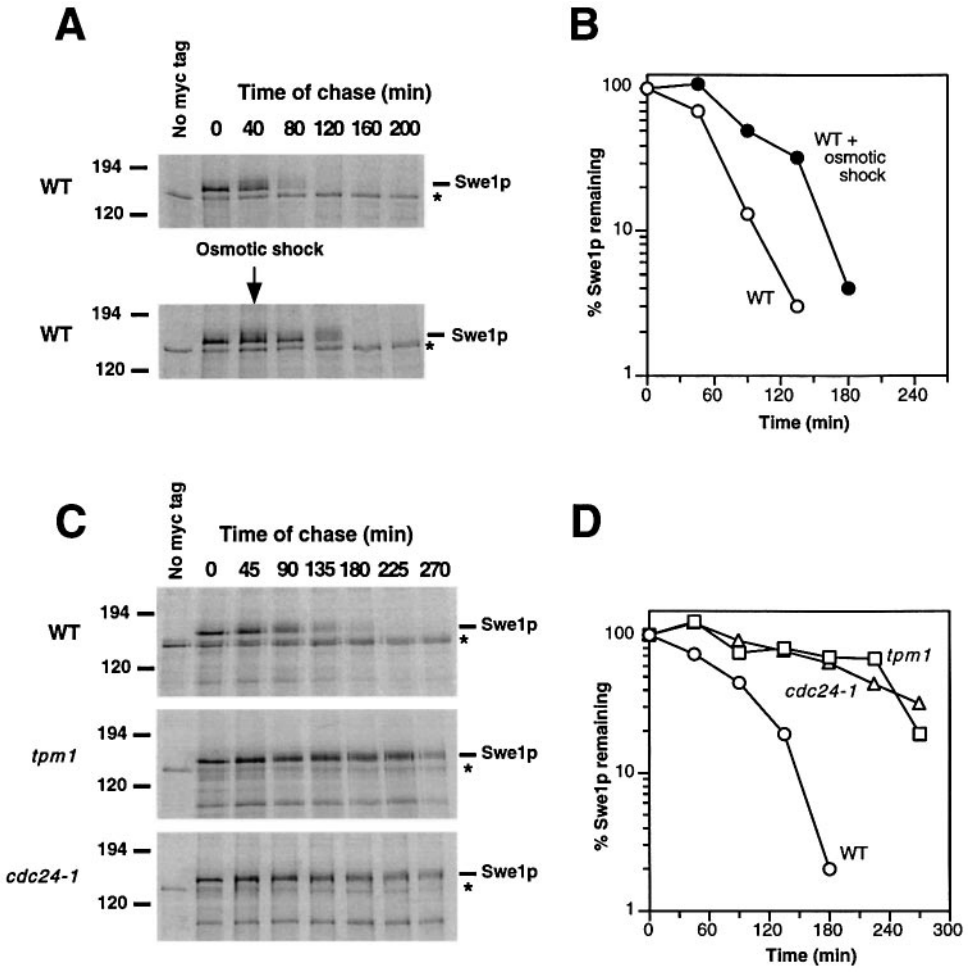

Fig. 3. Stabilization of Swe1p by the morphogenesis checkpoint. (**A**) Pulse–chase analysis of Swe1p stability in wild-type (RSY136) cells at 30°C. Top panel: no actin perturbation. Bottom panel: an osmotic shock (NaCl at 0.4 M final concentration) was applied at 40 min of chase, leading to a transient stabilization of Swe1p. The asterisk indicates a labeled band that is present in cells lacking Swe1p-myc (left lanes) and binds to protein A beads used for immunoprecipitation. Molecular weight markers (kDa) are indicated to the left of the panels. (**B**) Quantitation of the experiment shown in (A). (**C**) Pulse–chase analysis of Swe1p stability in wild-type (RSY136, top), *tpm1* (RSY204, middle) and *cdc24-1* (RSY138, bottom) cells. Cells were grown at 23°C and shifted to 37°C 2 h prior to the pulse–chase regimen, which was performed at 37°C. The asterisk indicates a labeled band that is present in cells lacking Swe1p-myc (left lanes) and binds to protein A beads used for immunoprecipitation. Molecular weight markers (kDa) are indicated to the left of the panels. (**D**) Quantitation of the experiment shown in (C).

initial degradation in the semi-log plots). Secondly, the rate of Swe1p-myc degradation in unperturbed cells, while considerably more rapid than that in cells undergoing a checkpoint response, was nevertheless surprisingly slow, taking ~2 h to degrade the majority of Swe1p-myc. This contrasts with the instability of Swe1p-myc that can be inferred from the immunoblots of synchronized cells (Figure 2A), where Swe1p-myc declined from peak to barely detectable levels in 30 min. One simple explanation for these observations might be that Swe1p degradation is cell-cycle regulated, so that the rate of Swe1p degradation in asynchronous cells (monitored in the pulse–chase experiment) reflects the rate at which cells in the population pass the cell cycle stage at which Swe1p is degraded, while the rate of Swe1p degradation in synchronized cells (monitored in the immunoblot experiment) more closely reflects the true instability of Swe1p at that stage.

One potentially complicating factor in examining whether Swe1p degradation is cell-cycle regulated is the possibility that there exists a feedback loop in which Swe1p degradation is stimulated by Cdc28p activity (see below). If activation of Cdc28p triggers Swe1p degradation, then inhibition of Cdc28p by Swe1p would cause Swe1p stabilization. Since we use a pulse of Swe1p overproduction to label detectable quantities of Swe1p for the pulse–chase experiment, there is the danger that this aspect of the protocol might stabilize Swe1p artifactually. To avoid this, we used a strain containing the $CDC28^{Y19F}$ mutant, rendering it resistant to Swe1p.

To address whether Swe1p degradation is cell-cycle regulated, we performed pulse–chase analysis of cells arrested in G_1 (with mating pheromone) or G_2/M phase (with nocodazole, which blocks spindle assembly). Quantification of cell morphologies confirmed >75% arrest both prior to the pulse and following the chase. Swe1p-myc was stable in G_1-arrested cells (half-life 90 min), but unstable in G_2/M-arrested cells (half-life 14 min; Figure 4). Thus, Swe1p stability is indeed cell-cycle regulated.

In addition to differences in Swe1p-myc stability, these experiments revealed differences in Swe1p-myc modific-

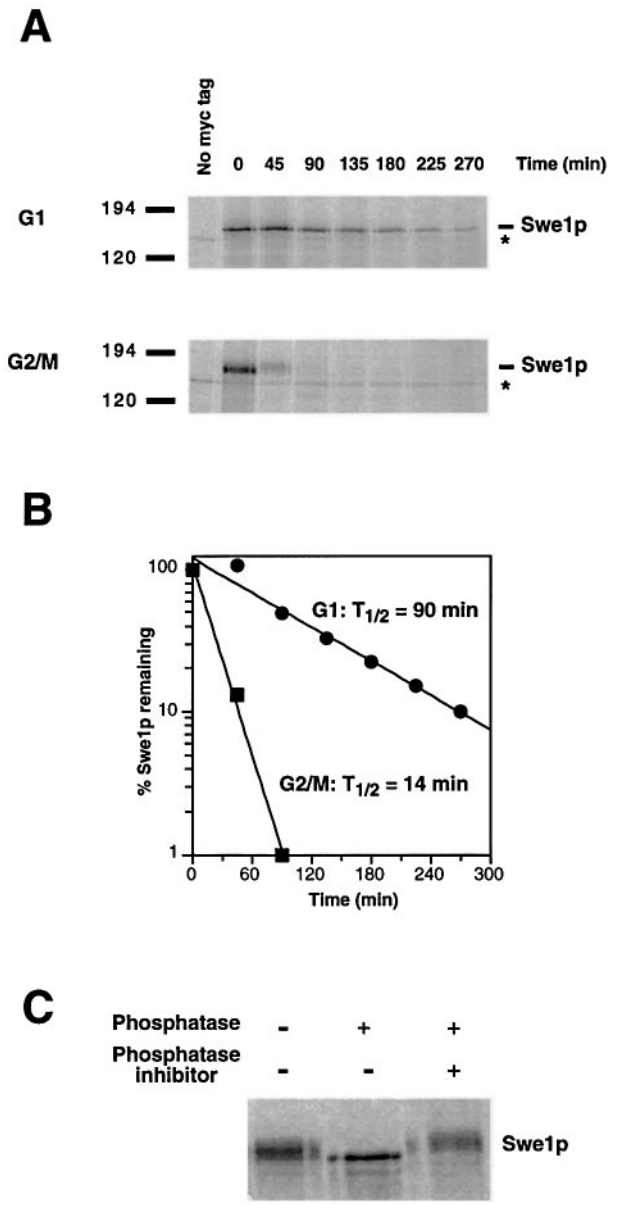

Fig. 4. Cell-cycle regulation of Swe1p stability. (**A**) Pulse–chase analysis of Swe1p stability in *CDC28*^{Y19F} cells (RSY342) arrested in G_1 or in G_2/M. α-Factor (50 ng/ml, top panel) or nocodazole (15 μg/ml, bottom panel) were added to the cells 3 h prior to the pulse–chase regimen and maintained at the same concentrations throughout. The asterisk indicates a labeled band that is present in cells lacking Swe1p-myc (left lanes) and binds to protein A beads used for immunoprecipitation. Molecular weight markers (kDa) are indicated to the left of the panels. (**B**) Quantitation of the experiment shown in (A). (**C**) Immunoprecipitates of Swe1p from an asynchronous culture, containing slower mobility forms of Swe1p, were either mock-treated (left), or treated with potato acid phosphatase (middle) or phosphatase in the presence of 10 mM sodium orthovanadate (right).

ation in cells arrested at different cell-cycle stages. While Swe1p-myc migrated as a tight band in G_1-arrested cells, it displayed several slower migrating species in G_2/M cells (Figure 4; see also previous figures). Phosphatase treatment of the immunoprecipitated Swe1p-myc caused the collapse of the slower migrating species to a single band similar to the Swe1p-myc from G_1 cells (Figure 4C), suggesting that the mobility difference is due to phosphorylation. Together, the data show that Swe1p-myc is moderately stable during G_1, and becomes hyperphosphorylated and quite unstable by G_2/M. It is not clear from this correlation whether Swe1p-myc phosphorylation is causally related to its degradation, but we note that Swe1p-myc does appear to undergo phosphorylation even under checkpoint-inducing conditions, when the protein is stable (Figures 2 and 3). Thus, there is no consistent correlation between Swe1p-myc phosphorylation (as visualized by the gel mobility shift) and Swe1p-myc degradation.

Cdc28p activity is required for Swe1p-myc degradation

The finding that Swe1p-myc was stable in G_1 but not in G_2/M phase prompted us to investigate whether there was a requirement for Cdc28p activity to trigger Swe1p-myc degradation. To this end, we tested whether the G_2 arrest caused by overproduction of Swe1p-myc (and consequent phosphorylation and inhibition of Cdc28p) was sufficient to stabilize Swe1p-myc in the absence of checkpoint induction. For this experiment, cells were induced to express the *GAL1*-regulated Swe1p-myc for 3 h prior to the pulse–chase regime (as opposed to 10 min in previous experiments). This caused a G_2 arrest with the characteristic highly elongated bud morphology previously described for cells lacking Clb1p–Cdc28p and Clb2p–Cdc28p activity, as occurs upon Swe1p overexpression (Booher *et al*., 1993; Lew and Reed, 1993). Galactose medium was then used throughout to maintain Swe1p-myc expression and cell cycle arrest. Under these conditions, Swe1p-myc was stable (Figure 5). A caveat to this experiment is that simply overproducing Swe1p-myc to these high levels might titrate out a limiting factor required for Swe1p-myc degradation, so that the stability observed arises due to the excess of Swe1p-myc rather than the G_2 arrest. To distinguish these options, we performed a parallel experiment using a *CDC28*^{Y19F} mutant strain, resistant to Swe1p. In this strain, Swe1p-myc was once again unstable (although the Swe1p-myc overexpression did result in a somewhat slower degradation; Figure 5), indicating that a simple excess of Swe1p-myc cannot account for its stability in the wild-type strain. Thus, Swe1p-myc-mediated inhibition of Cdc28p can trigger Swe1p-myc stabilization in the absence of a checkpoint stimulus, suggesting that Clb–Cdc28p activity is required for Swe1p degradation.

We confirmed this result using overexpression of Sic1p, a stoichiometric inhibitor of Clb–Cdc28p complexes, as an alternative method to inhibit Cdc28p. A strain was constructed containing multiple copies of a *GAL–SIC1* construct, in addition to the *GAL–SWE1myc* used for the pulse–chase analysis and a *CDC28*^{Y19F} allele (see Materials and methods). Addition of galactose for 3 h resulted in accumulation of Sic1p and consequent arrest of the cell cycle with the characteristic multiple elongated buds described for arrest without Clb–Cdc28p activity. Pulse–chase analysis demonstrated that Swe1p-myc was stable in these cells (Figure 5). Thus, Swe1p degradation is blocked in cells whose Clb–Cdc28p complexes have been inhibited by either Swe1p or Sic1p. We conclude that Clb–Cdc28p activity is required (directly or indirectly) for triggering Swe1p degradation.

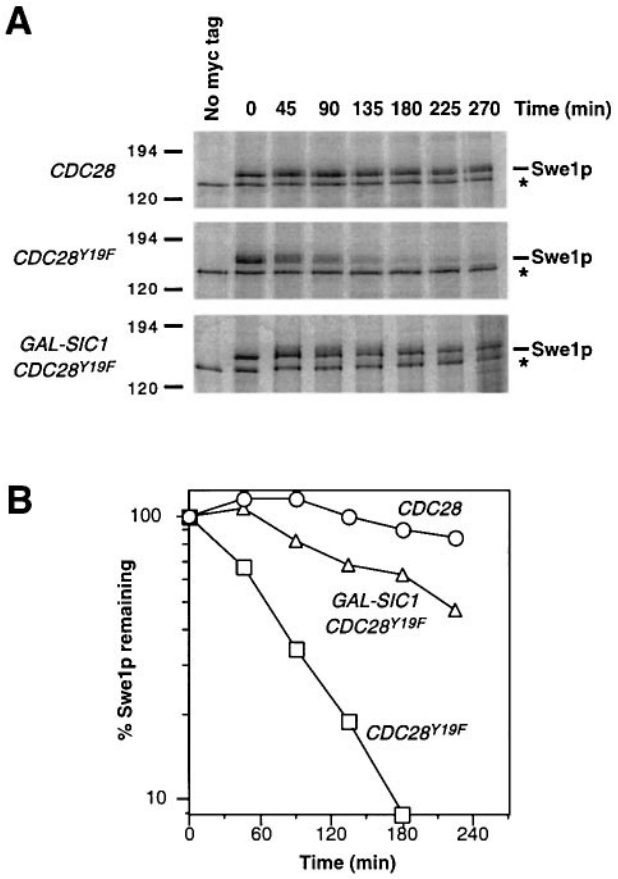

Fig. 5. Clb–Cdc28p kinase is required for Swe1p degradation. (**A**) Pulse–chase analysis of Swe1p stability in cells overexpressing Swe1p. For these experiments, galactose was added to the cells 3 h prior to the pulse–chase regimen to induce Swe1p overexpression, and maintained throughout. Top panel: wild-type (RSY136) cells—these cells arrest with low Clb1p-2p–Cdc28p kinase as a result of the Swe1p overexpression. Middle panel: *CDC28*^{Y19F} (RSY342) cells—these cells fail to arrest (although they do pause transiently in G_2). Bottom panel: *CDC28*^{Y19F} *GAL–SIC1* (RSY357) cells—these arrest with low Clb1p-6p–Cdc28p kinase as a result of the Sic1p overexpression. Swe1p was stable in the arrested cells but not in the *CDC28*^{Y19F} cells, even though these also overexpress Swe1p. The asterisk indicates a labeled band that is present in cells lacking Swe1p-myc (left lanes) and binds to protein A beads used for immunoprecipitation. Molecular weight markers (kDa) are indicated to the left of the panels. (**B**) Quantitation of the experiment shown in (A).

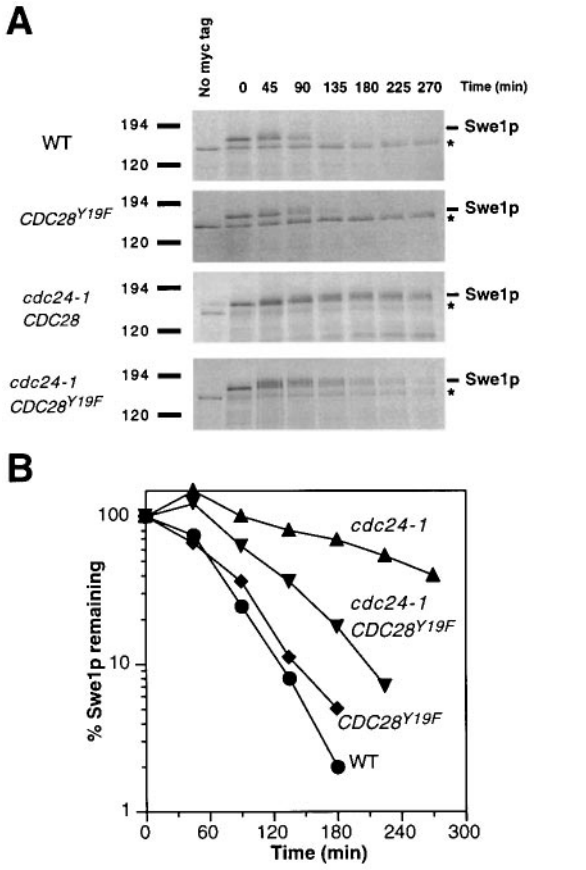

Fig. 6. Full stabilization of Swe1p by the morphogenesis checkpoint requires the checkpoint-induced G_2 delay. (**A**) Pulse–chase analysis of Swe1p stability in wild-type (RSY136, top panel), *CDC28*^{Y19F} (RSY342, second panel), *cdc24-1* (RSY138, third panel) and *cdc24-1 CDC28*^{Y19F} (RSY195, bottom panel) cells. Cells were grown at 23°C and shifted to 37°C 2 h prior to the pulse–chase regimen, which was performed at 37°C. The asterisk indicates a labeled band that is present in cells lacking Swe1p-myc (left lanes) and binds to protein A beads used for immunoprecipitation. Molecular weight markers (kDa) are indicated to the left of the panels. (**B**) Quantitation of the experiment shown in (A).

Maintenance of the G_2 arrest is required for full stabilization of Swe1p by the morphogenesis checkpoint

The finding that G_2-arrested cells contained stable Swe1p-myc raised the question of whether the Swe1p-myc in checkpoint-arrested cells was stabilized directly by a checkpoint-mediated pathway, or indirectly through the G_2 arrest that accompanied the checkpoint. To distinguish these options, we compared the stability of Swe1p-myc in *cdc24-1* cells containing wild-type *CDC28* or the *CDC28*^{Y19F} mutant. In both cases, the *cdc24-1* mutation prevents actin polarization, triggering the checkpoint. However, cells containing the *CDC28*^{Y19F} mutant fail to arrest in response to the Swe1p induced by the checkpoint, and continue through mitosis after a small delay (Lew and Reed, 1995). Swe1p-myc was degraded in control wild-type and *CDC28*^{Y19F} strains, but stable in the *cdc24-1* mutant incubated at the restrictive temperature (Figure 6). In the *cdc24-1 CDC28*^{Y19F} strain, we obtained an intermediate result: Swe1p-myc was degraded more rapidly than in *cdc24-1* cells, but seemed more stable than in wild-type cells (Figure 6). This result was highly reproducible, and shows that the G_2 arrest contributes to at least a part of the checkpoint-induced stabilization of Swe1p-myc. Possible explanations for the intermediate stability of Swe1p-myc in this experiment are considered in the Discussion.

As an alternative means to address the same question, we monitored the behavior of Swe1p-myc expressed from its own promoter in synchronized cells undergoing a checkpoint response to *cdc24-1*. Once again, we compared cells containing wild-type *CDC28* or the *CDC28*^{Y19F} mutant. As before, Swe1p-myc levels remained elevated in checkpoint-arrested *cdc24-1* cells (Figure 7). However, in *cdc24-1* cells that failed to arrest (due to the *CDC28*^{Y19F} mutant), Swe1p-myc levels peaked and then declined (Figure 7). In multiple experiments, we never observed a complete elimination of Swe1p-myc in these cells, but it is unclear whether this reflects a partial stabilization of Swe1p or simply the imperfect synchrony of the cell

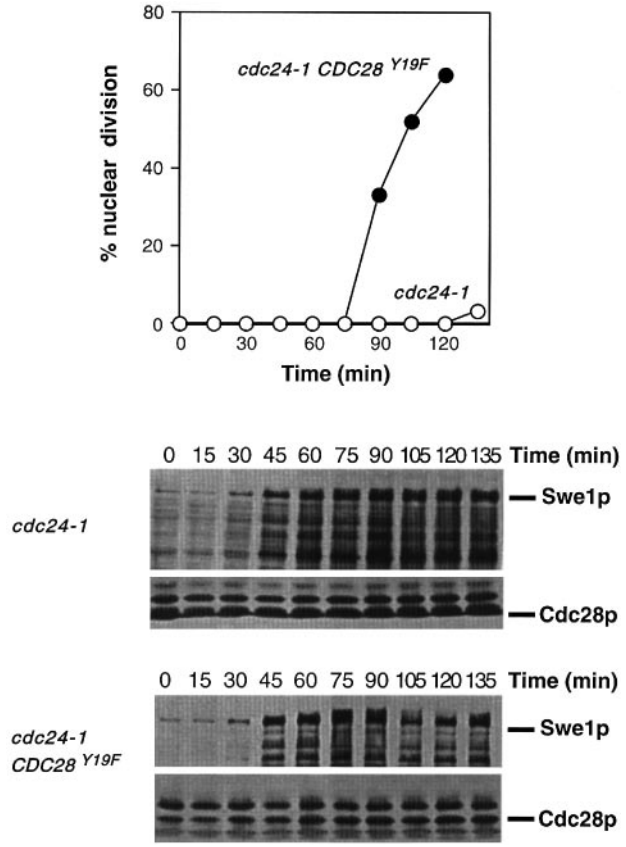

Fig. 7. Swe1p is degraded in cells that override the morphogenesis checkpoint G_2 delay. Pheromone arrest–release synchrony of *cdc24-1* (RSY258) and *cdc24-1 CDC28*^{Y19F} (RSY310) cells. Cells were grown at 23°C, arrested in G_1 with pheromone and released from the arrest at 37°C. The cumulative percentage of cells that underwent chromosome separation is plotted for the same samples shown in the immunoblots. The *cdc24-1 CDC28*^{Y19F} cells failed to delay nuclear division despite the inability to polarize actin.

population. Regardless, this experiment confirms the results from the pulse–chase analysis and demonstrates that Swe1p-myc is (at least partly) degraded as cells progress through mitosis, even if they have triggered the morphogenesis checkpoint.

Discussion

We have shown previously that *SWE1* is essential for the G_2 delay or arrest triggered by the morphogenesis checkpoint in response to a variety of perturbations that affect actin organization in budding yeast (Lew and Reed, 1995; Sia *et al*., 1996; McMillan *et al*., 1998). Although *SWE1* transcription was regulated both during the cell cycle and in response to the checkpoint, we found that transcriptional control was not essential for the Swe1p-dependent G_2 delay under checkpoint conditions, implying the existence of other regulatory strategies (Sia *et al*., 1996). In this study, we have investigated the behavior of Swe1p both in unperturbed cells and in cells responding to the checkpoint. We found that Swe1p degradation was regulated during the cell cycle, and that Swe1p was stabilized in cells responding to the checkpoint. This was true in response to three very different checkpoint-inducing perturbations (osmotic shock, *cdc24-1* mutants and *tpm1* mutants), supporting our conclusion that these varied perturbations all trigger the same checkpoint response.

Cell cycle control of Swe1p stability

Swe1p abundance, phosphorylation and stability all varied as a function of cell cycle progression. Swe1p levels were low in G_1-arrested cells, and increased to a peak in S or early G_2 phase after cells had formed buds. This peak is significantly delayed (30 min) relative to the peak of *SWE1* mRNA accumulation, which occurs in late G_1 prior to bud emergence (Lim *et al*., 1996; Ma *et al*., 1996; Sia *et al*., 1996), suggesting that Swe1p is relatively stable at this stage of the cell cycle. However, Swe1p levels decline precipitously during later G_2 and M phase, suggesting that Swe1p becomes quite unstable at this stage. Pulse–chase experiments on cell-cycle-arrested cells confirmed that Swe1p was stable (half-life 90 min) in G_1-arrested cells, but unstable (half-life 14 min) in G_2/M-arrested cells. Thus, Swe1p joins a growing list of key cell-cycle regulators, including cyclins, Cdk inhibitors and regulators of anaphase onset and DNA replication (King *et al*., 1996), that oscillate in stability during the cell cycle.

A potential feedback loop involving Swe1p degradation

Inhibition of Clb–Cdc28p activity through Sic1p or Swe1p overexpression led to Swe1p stabilization. This supports a model in which activation of Clb–Cdc28p complexes targets Swe1p for degradation. Since Swe1p is an inhibitor of Clb–Cdc28p complexes, its degradation could contribute to the activation of these complexes, revealing a potential feedback loop operating during G_2/M phase in budding yeast (Figure 8A). Similar feedback loops have been proposed involving *SWE1* transcription in budding yeast (Figure 8A; Sia *et al*., 1996), and involving wee1 phosphorylation in fission yeast (Figure 8B; reviewed by Dunphy, 1994; Lew and Kornbluth, 1996). In each case, activation of cyclin–Cdk complexes at the G_2/M transition shuts down the kinases that inhibit those complexes (in the case of Swe1p, through transcriptional repression and protein degradation; in the case of wee1, through inhibitory phosphorylation). Such feedback loops have been proposed to accelerate or 'sharpen' the G_2/M transition in unperturbed cells (Dunphy, 1994; Lew and Kornbluth, 1996). An equally important though less frequently discussed consequence of these feedback loops is that checkpoint mechanisms that restrain activation of cyclin–Cdk complexes can call upon the resulting continued activity of the inhibitory kinases (Swe1p or wee1) to aid in maintaining low cyclin–Cdk activity.

Swe1p phosphorylation

How does Clb–Cdc28p activity target Swe1p for degradation? One possibility is suggested by the provocative observation that Swe1p was modified into progressively slower migrating forms (by SDS–PAGE analysis) as cells traversed the cell cycle. Phosphatase treatment converted the slower migrating forms back to the faster migrating form seen in G_1 cells, demonstrating that the differences in gel migration were the result of Swe1p phosphorylation. Thus, Clb–Cdc28p activation could lead, directly or indirectly, to phosphorylation of Swe1p, which may target Swe1p for degradation. There is a precedent from studies

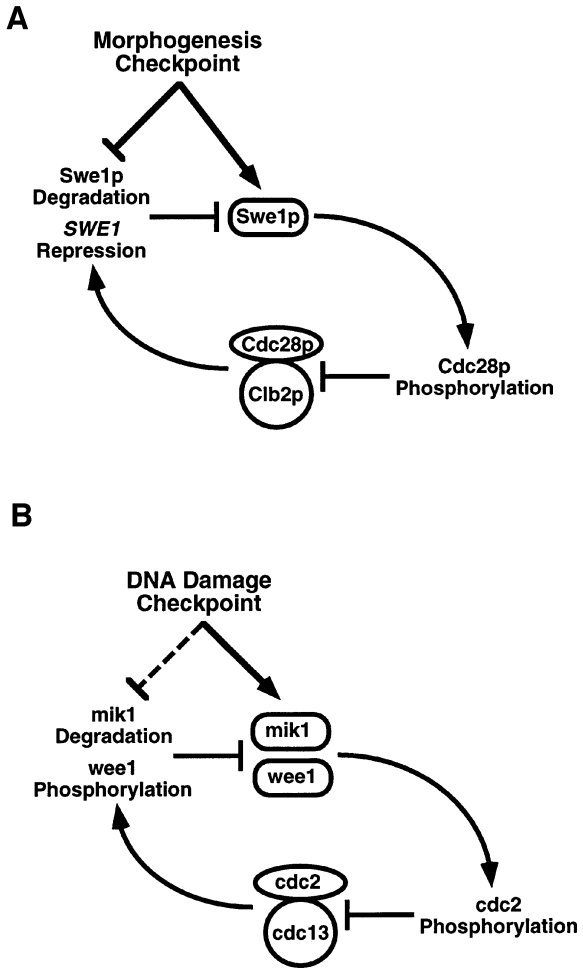

Fig. 8. Summary and model. (**A**) Interplay between Swe1p and Clb1p-2p–Cdc28p in budding yeast. The checkpoint may regulate Swe1p degradation and/or other aspects of Swe1p function directly (see text for details). (**B**) Interplay between wee1 and mik1 (both homologous to Swe1p) and cdc13–cdc2 in fission yeast, illustrated for comparison. The pathways involving mik1 degradation are purely hypothetical (see text).

in vertebrate cells for cyclin–cdc2-induced phosphorylation of Wee1 (Tang *et al*., 1993; Dunphy, 1994; McGowan and Russell, 1995), although in these cases phosphorylation was associated with inhibition of Wee1 activity rather than its degradation. In addition, we have shown recently that Swe1p degradation involves its ubiquitination by a complex containing Cdc34p, Cdc53p, Skp1p and Met30p (Kaiser *et al*., 1998). Previous studies on the degradation of the Cdk inhibitor Sic1p showed that phosphorylation of Sic1p by Cln–Cdc28p complexes targeted it for ubiquitination by a similar (though distinct) Cdc34p-containing complex (Feldmann *et al*., 1997; Skowyra *et al*., 1997). Thus, it is tempting to speculate that Clb–Cdc28p-induced phosphorylation might target Swe1p similarly for Cdc34p-mediated ubiquitination and subsequent degradation.

Although Swe1p phosphorylation preceded its degradation in unperturbed cells, phosphorylation also occurred in checkpoint-arrested cells where Swe1p was stable. Phosphorylation was detected through changes in Swe1p migration, and it is possible that different sites on Swe1p were phosphorylated in unperturbed versus checkpoint-arrested cells; perhaps only the sites phosphorylated in unperturbed cells are involved in targeting Swe1p for degradation. Alternatively, the checkpoint may regulate the ubiquitination or degradation machinery so that it no longer recognizes phosphorylated Swe1p. Finally, it remains possible that Swe1p phosphorylation is unconnected to its degradation, but rather influences some other property such as Swe1p activity. Distinguishing these possibilities will require mapping of the phosphorylation sites on Swe1p and mutagenesis to generate non-phosphorylatable mutants.

Checkpoint control of Swe1p stability

Swe1p accumulated to high levels in cells arrested by the morphogenesis checkpoint, and Swe1p was very stable (half-life >4 h) in these cells. This suggests that the checkpoint stabilizes Swe1p, promoting its accumulation and consequent cell cycle delay in G_2. However, a G_2 arrest independent of the checkpoint also led to stabilization of Swe1p, raising the possibility that the G_2 arrest triggered by the checkpoint causes Swe1p stabilization. To address this, we monitored Swe1p behavior in cells that had triggered the checkpoint but were unable to maintain a G_2 arrest. In these cells, Swe1p was (at least partly) degraded as the cells progressed through mitosis, showing that the G_2 arrest induced by the checkpoint is necessary to maintain Swe1p stability. Thus, Swe1p stabilization can be viewed as part of a feedback loop which contributes to the checkpoint-mediated G_2 arrest by keeping Swe1p levels high (Figure 8A).

If stabilization of Swe1p by the checkpoint is largely indirect (through the G_2 arrest), then what is it that initially triggers the G_2 arrest in these cells? One possibility is that an initial stabilization of Swe1p, triggered directly by the checkpoint, leads to a G_2 arrest which is then amplified by the feedback loop. In this scenario, the checkpoint may be able to protect Swe1p in G_2 cells (with moderate Clb–Cdc28p activity) from degradation, but unable to protect Swe1p in mitotic cells (with high Clb–Cdc28p activity) from degradation. This hypothesis is attractive in that it provides an explanation for the apparently intermediate Swe1p stability observed in *cdc24-1 CDC28*^{Y19F} cells (Figure 6). Perhaps this result reflects selective stabilization of Swe1p in pre-mitotic cells. An alternative, and not mutually exclusive, possibility would be that the checkpoint initially enhances Swe1p activity, leading to inhibition of Clb–Cdc28p and consequent Swe1p stabilization. These possibilities are indicated by the bifurcating arrows in Figure 8A.

The uncertainty regarding the issue of whether Swe1p stability is a primary or secondary consequence of the checkpoint is mirrored by a similar uncertainty in the interpretation of data concerning wee1 and cdc25 regulation by the DNA damage and DNA replication checkpoints (Furnari *et al*., 1997; O'Connell *et al*., 1997; Peng *et al*., 1997; Sanchez *et al*., 1997; Boddy *et al*., 1998). Although checkpoint kinases were shown to phosphorylate wee1 or cdc25 during the checkpoint arrest, it has yet to be determined whether such phosphorylations would persist if the G_2 arrest were bypassed. Indeed, it could be argued that once cells have made the commitment to enter mitosis, it is important to eliminate any Cdk-inhibitory pathways that might remain active from the preceding interphase,

Table I. Yeast strains

Strain	Relevant genotype
DLY1	MAT**a** *bar1*
DLY657	MAT**a** *bar1 cdc24-1*
DLY690	MAT**a** *bar1 cdc24-1 swe1::LEU2*
DLY1028	MAT**a** *bar1 swe1::LEU2*
RSY136	MAT**a** *bar1 GAL-SWE1myc::URA3*
RSY138	MAT**a** *bar1 cdc24-1 GAL-SWE1myc::URA3*
RSY195	MAT**a** *bar1 cdc24-1 CDC28^{Y19F}::TRP1 GAL-SWE1myc::URA3*
RSY204	MATα *tpm1::URA3 GAL-SWE1myc::URA3*
RSY206	MAT**a** *bar1 SWE1myc::URA3::GAL-SWE1*
RSY258	MAT**a** *bar1 cdc24-1 SWE1myc::URA3*
RSY310	MAT**a** *bar1 cdc24-1 CDC28^{Y19F}::TRP1 SWE1myc::URA3*
RSY311	MAT**a** *bar1 SWE1myc::URA3*
RSY336	MAT**a** *bar1 tpm1::URA3 SWE1myc::URA3*
RSY342	MAT**a** *bar1 CDC28^{Y19F}::TRP1 GAL-SWE1myc::URA3*
RSY357	MAT**a** *bar1 CDC28^{Y19F}::TRP1 GAL-SWE1myc::URA3 GAL-SIC1::LEU2*

in order to avoid 'mixed signals' that might impair mitotic progression. This would explain the apparently ubiquitous feedback loops ensuring a full activation of cyclin–Cdk complexes in mitotic cells. Demonstrating the direct chain of events whereby individual checkpoints affect cell cycle progression is made technically very demanding by the presence of these feedback loops, and remains a major challenge for the field.

Functional consequences of the control of Swe1p degradation

The regulation of Swe1p stability we describe here is functionally important for the operation of the morphogenesis checkpoint at two levels. First, we recently have shown that the responsiveness of cells to actin perturbation declines as they progress through the cell cycle, and that this decline is due (at least in part) to the decline in Swe1p abundance (McMillan *et al*., 1998). Thus, instability of Swe1p in the unperturbed cycle is important for limiting the window of the cell cycle within which cells will arrest in response to actin perturbation. Secondly, we have shown that the gene dosage of *SWE1*, and by implication the abundance of Swe1p, is critical for determining the duration of the G_2 delay enacted in response to actin perturbation (Sia *et al*., 1996). Thus, stabilization of Swe1p contributes to the length of the G_2 delay introduced by the checkpoint, ensuring that nuclear division remains coordinated with bud formation. Taken together, the data reported here combined with previous studies suggest that periodic transcription and proteolysis of Swe1p during the unperturbed cell cycle limits the abundance of Swe1p in G_2, reducing its effectiveness as a cell cycle inhibitor [in contrast to fission yeast, where wee1 transcript levels are constitutive and protein abundance is relatively constant (Aligue *et al*., 1997), and wee1 is a highly effective cell-cycle inhibitor]. Upon perturbation of actin organization, Swe1p is stabilized, and cells that are still early in the cell cycle (and hence still need polarized actin to complete bud formation) contain sufficient Swe1p to trigger G_2 arrest. The G_2 arrest allows time for recovery of actin polarity and completion of bud formation, following which the cells can proceed through mitosis.

Implications for other systems

A morphogenesis checkpoint has not yet been described in organisms other than budding yeast, but control of cdc2 tyrosine phosphorylation is important for both the DNA replication checkpoint and the DNA damage checkpoint in other organisms (see Introduction). In fission yeast, two tyrosine kinases, wee1 and mik1 (both equally homologous to Swe1p), are involved in cdc2 regulation (Lundgren *et al*., 1991). Wee1 levels appear to remain constant during a checkpoint arrest, but very recently it was reported that mik1 levels increase dramatically following DNA damage (Boddy *et al*., 1998), perhaps due to regulation of mik1 stability (Figure 8B). Given the widespread conservation of mitotic control pathways among eukaryotes, it seems likely that the capacity to regulate the destruction of Swe1p homologs will prove relevant to various situations.

Conclusion

Regulated degradation of cell cycle regulators has taken center stage in recent years as a key element of cell cycle control. We now show that Swe1p also undergoes such regulated degradation. Furthermore, stabilization of Swe1p contributes to the cell cycle arrest caused by the morphogenesis checkpoint in budding yeast. Future studies must address the detailed mechanism underlying control of Swe1p stability, and examine the applicability of this form of regulation to other systems.

Materials and methods

Yeast strains, growth conditions and cell synchrony

The yeast strains used in this study are listed in Table I: all are in the BF264-15DU background (*ade1, his2, leu2-3,112, trp1-1^a, ura3Δns*). The *GAL1–SWE1myc* and *SWE1*myc constructs were described recently (McMillan *et al*., 1998). Strains RSY206 and RSY311 both contain *SWE1myc*, but differ in that RSY206 contains a *GAL–SWE1* gene adjacent to the integrated *SWE1myc*, while RSY311 does not: these strains behave identically when grown on glucose media, as in the experiments reported here. To overexpress Sic1p, we used a YIpG2::SIC1 plasmid constructed and generously provided by Peter Kaiser (The Scripps Research Institute, La Jolla, CA). In brief, the *SIC1* open reading frame was PCR amplified with appropriate cloning sites and inserted downstream of the *GAL1* promoter in YIpG2 (Ghiara *et al*., 1991; Stueland *et al*., 1993). Following digestion with *Bst*EII (which cuts at a unique site within the *LEU2* marker), this plasmid was transformed into RSY342. Two classes of transformants were obtained: one class showed the heterogeneous phenotype described previously (Nugroho and Mendenhall, 1994) for single-copy *GAL–SIC1*, while the other exhibited cell-cycle arrest with multiple elongated buds on galactose, indicative of multiple *GAL–SIC1* integrants (Schwob *et al*., 1994). To integrate the *CDC28^{Y19F}* allele, a 740 bp *Xho*I–*Dra*I fragment of *CDC28^{Y19F}* containing the promoter + N-terminal portion of the Cdc28p-Y19F open

reading frame was isolated from pSF38 (Sorger and Murray, 1992), and cloned into *Sal*I–*Sma*I-cut YIplac204 [a *TRP1*-marked integrating vector (Geitz and Sugino, 1988); *Xho*I–*Sal*I and *Dra*I–*Sma*I junctions are compatible]. The plasmid was cut with *Afl*II to target integration at the *CDC28* locus, yielding a $CDC28^{Y19F}$ driven from its own promoter and an adjacent N-terminal fragment of *CDC28*. Correct integration was confirmed by resistance to Swe1p overexpression, and by PCR amplification of genomic *CDC28* using the oligonucleotides 5′-AAACGCCAAAAATAAAAACGAAC-3′ and 5′-AATTGAGGCCCCAGCATACA-3′, followed by restriction analysis with *Nde*I, which cuts at the start of the $CDC28^{Y19F}$ from pSF38, but does not cut wild-type *CDC28*.

Cells were grown in rich medium (YEPD: 1% yeast extract, 2% bacto-peptone, 2% dextrose, 0.01% adenine; or YEPS, containing 2% sucrose instead of 2% dextrose) at 30°C, except for experiments involving *cdc24-1* strains, for which cells were grown at 23°C and shifted to 37°C as indicated. For pheromone arrest–release experiments, exponentially growing cells ($2–5\times10^6$ cells/ml) in YEPD were incubated with 20–25 ng/ml α-factor for 2–3 h, harvested by centrifugation and resuspended in fresh YEPD to release the α-factor-induced cell cycle block. *bar1* strains were used in all of the α-factor synchrony experiments. Aliquots of cells were fixed with 70% ethanol, stained with 0.4 μg/ml 4′,6′-diamidino-2-phenylindole (DAPI: Sigma Chemical Co., St Louis, MO) (Pringle *et al*., 1991) and examined microscopically to determine the percentage of cells that had formed buds or completed anaphase. For pulse–chase experiments (see below), cells were grown in YEPS, and induced to express *SWE1* by addition of galactose to 2% final concentration. Where indicated, cell synchrony or arrest was quantitated by examination of cell morphology in aliquots of cells fixed just before the pulse or at various times during the chase.

Yeast lysates and immunoblotting

Yeast cells were washed with ice-cold H_2O and harvested by centrifugation. Pellets were stored frozen at –80°C. Lysates were made by resuspending pellets in a buffer containing 50 mM Tris–HCl (pH 7.5), 150 mM NaCl, 5 mM EDTA, 1% NP-40, 1 mM sodium pyrophosphate, 1 mM phenylmethylsulfonyl fluoride (PMSF), 1 mM sodium orthovanadate and 2 μg/ml each of aprotinin, pepstatin A and leupeptin, and vortexing with acid-washed glass beads. Lysates were clarified by centrifugation (8 min, 14 000 r.p.m. in an Eppendorf centrifuge), and the protein concentration was determined by the BioRad assay. An aliquot of 50 μg of total protein (per gel lane) from each lysate was mixed with hot (95°C) 2× sample loading buffer (final concentrations 62.5 mM Tris–HCl pH 6.8, 1% SDS, 25% glycerol, 355 mM β-mercaptoethanol, 0.01% bromophenol blue) and incubated at 95°C for 5 min prior to running on 8% polyacrylamide gels. Following standard SDS–PAGE, proteins were transferred to Immobilon transfer membrane (Millipore Corp., Bedford, MA) and the membrane was cut in two. The upper half was immunoblotted with anti-myc antibody 9E10 (Santa Cruz Biotechnology, Inc., Santa Cruz, CA) and the bottom half with anti-PSTAIRE antibody (this recognizes Cdc28p and Pho85p). Membranes were first blocked in 5% dry milk in phosphate-buffered saline with 0.1% Tween (PBS-Tween). Primary antibodies were used at 1:1000 dilution (anti-myc) or 1:25 000 dilution (anti-PSTAIRE) in 1% milk/PBS-Tween. Secondary antibody (horseradish peroxidase-conjugated goat anti-mouse; Jackson Immunoresearch Laboratories, Inc., West Grove, PA) was used at 1:2500 dilution in PBS-Tween. All incubations were carried out for 1 h and separated by three washes with PBS-Tween. Blots were developed using the Renaissance Western Blot Chemiluminescence Reagent Plus (NEN Life Sciences Products, Boston, MA).

Pulse–chase analysis of Swe1p-myc stability

Cells containing the *GAL1-SWE1myc* construct were grown in YEPS and induced to express Swe1p-myc by addition of 2% galactose for 10 min. Cells were then harvested by centrifugation, resuspended at 10^8 cells/ml in labeling medium [yeast nitrogen base minus methionine, 2% sucrose and 2% galactose with 0.25 mCi/ml (0.183 mM) Trans^{35}S-Label (ICN)] and incubated for a further 10 min to label newly synthesized proteins with [^{35}S]methionine/cysteine. Labeled cells were collected by filtration, washed with pre-warmed YEPD, and resuspended at 3×10^7 cells/ml in fresh YEPD supplemented with 3 mM methionine and 0.5% casamino acids to prevent further labeling. Incubation was continued, and aliquots of cells were diluted into ice-cold 10 mM NaN_3, harvested by centrifugation, washed with ice-cold 10 mM NaN_3 and frozen at –80°C. For the experiments shown in Figure 4, the protocol was modified as follows: α-factor (50 ng/ml final concentration) or nocodazole (15 μg/ml final concentration) was added 3 h prior to galactose addition, and subsequent incubations were performed in media containing the same concentration of α-factor or nocodazole. For the experiments of Figure 5, the protocol was modified as follows: galactose was added 3 h prior to the pulse labeling, and the 'chase' was performed in YEPG (2% galactose) rather than YEPD. All incubations were at 30°C except for experiments involving *cdc24-1* strains, which were grown at 23°C and shifted to 37°C 2 h prior to the addition of galactose, and maintained at 37°C thereafter.

Cell pellets were lysed in ice-cold 50 mM Tris, pH 7.5, 5 mM EDTA, 1 mM sodium pyrophosphate, 150 mM sodium chloride, 1% NP-40, 1 mM sodium orthovanadate, 1 mM PMSF, 1 μg/ml leupeptin and 1 μg/ml pepstatin. Swe1p-myc was immunoprecipitated using the anti-c-Myc (9E10) antibody from lysates containing equal amounts of radioactive label, and the immunoprecipitates were washed three times with lysis buffer, boiled for 10 min in 1× SDS sample loading buffer and separated by SDS–PAGE in 8% polyacrylamide gels. Dried gels were exposed to Molecular Dynamics storage phosphor screen for 24–48 h, scanned on a Molecular Dynamics 445 SI PhosphorImager and analyzed with ImageQuant v1.2 software.

Phosphatase treatment

Swe1p-myc was immunoprecipitated from ^{35}S-labeled asynchronous cells as described above, washed three times with lysis buffer, and divided into three equal aliquots. Beads were resuspended in 40 mM PIPES, pH 6, 1 mM dithiothreitol, 6 mM PMSF, 40 μg/ml aprotinin and 20 μg/ml each of benzamidine, leupeptin and pepstatin (high concentrations of protease inhibitors were required to inhibit proteases contaminating the phosphatase preparation). Then 0.36 U of type II potato acid phosphatase (Sigma Chemical Co., St Louis, MO) was added and samples were incubated at 30°C for 30 min. Mock treatment was identical, but without adding phosphatase. Sodium orthovanadate (10 mM) was added to inhibit phosphatase activity, as indicated.

Flow cytometry

Cells were processed for flow cytometry as described (Haase and Lew, 1997), except that DNA was stained with 1 μM Sytox (Molecular Probes, Eugene, OR) in 50 mM Tris–HCl pH 8.0 instead of propidium iodide, and analyzed on the FL1 channel on a Becton-Dickinson FACScan. Nuclear division was quantitated using the same samples for microscopic examination; 200 cells were counted per time point.

Acknowledgements

We thank Peter Kaiser and Peter Sorger for plasmids, and Lynn Martinek and Mike Cook from the Duke Cancer Center Flow Cytometry Shared Resource for help with the flow cytometry. We thank Sally Kornbluth for critical reading of the manuscript, John McMillan for valuable advice, and the members of the Lew and Pringle labs for stimulating interactions. This work was supported by US Public Health Service grant GM53050 and by funds from the Searle Scholars Program/The Chicago Community Trust to D.J.L.

References

Adams,A.E.M. and Pringle,J.R. (1984) Relationship of actin and tubulin distribution to bud growth in wild-type and morphogenetic-mutant *Saccharomyces cerevisiae*. *J. Cell Biol*., **98**, 934–945.

Aligue,R., Wu,L. and Russell,P. (1997) Regulation of *Schizosaccharomyces pombe* wee1 tyrosine kinase. *J. Biol. Chem*., **272**, 13320–13325.

Amon,A., Surana,U., Muroff,I. and Nasmyth,K. (1992) Regulation of $p34^{CDC28}$ tyrosine phosphorylation is not required for entry into mitosis in *S.cerevisiae*. *Nature*, **355**, 368–371.

Blasina,A., Paegle,E.S. and McGowan,C.H. (1997) The role of inhibitory phosphorylation of cdc2 following DNA replication block and radiation-induced DNA damage in human cells. *Mol. Biol. Cell*, **8**, 1013–1023.

Boddy,M.N., Furnari,B., Mondesert,O. and Russell,P. (1998) Replication checkpoint enforced by kinases Cds1 and Chk1. *Science*, **280**, 909–912.

Booher,R.N., Deshaies,R.J. and Kirschner,M.W. (1993) Properties of *Saccharomyces cerevisiae* wee1 and its differential regulation of $p34^{CDC28}$ in response to G1 and G2 cyclins. *EMBO J*., **12**, 3417–3426.

Chowdhury,S., Smith,K.W. and Gustin,M.C. (1992) Osmotic stress and the yeast cytoskeleton: phenotype-specific suppression of an actin mutation. *J. Cell Biol*., **118**, 561–571.

Dunphy,W.G. (1994) The decision to enter mitosis. *Trends Cell Biol*., **4**, 202–207.

Elledge,S.J. (1996) Cell cycle checkpoints: preventing an identity crisis. *Science*, **274**, 1664–1672.

Feldmann,R.M.R., Correll,C.C., Kaplan,K.B. and Deshaies,R.J. (1997) A complex of Cdc4p, Skp1p and Cdc53p/Cullin catalyzes ubiquitination of the phosphorylated CDK inhibitor Sic1p. *Cell*, **91**, 221–230.

Furnari,B., Rhind,N. and Russell,P. (1997) Cdc25 mitotic inducer targeted by Chk1 DNA damage checkpoint kinase. *Science*, **277**, 1495–1497.

Geitz,R.D. and Sugino,A. (1988) New yeast–*Escherichia coli* shuttle vectors constructed with *in vitro* mutagenized yest genes lacking six base pair restriction sites. *Gene*, **74**, 527–534.

Ghiara,J.B., Richardson,H.E., Sugimoto,K., Henze,M., Lew,D.J., Wittenberg,C. and Reed,S.I. (1991) A cyclin B homolog in *S.cerevisiae*: chronic activation of the Cdc28 protein kinase by cyclin prevents exit from mitosis. *Cell*, **65**, 163–174.

Haase,S.B. and Lew,D.J. (1997) Flow cytometric analysis of DNA content in budding yeast. *Methods Enzymol*., **283**, 322–332.

Hartwell,L.H. and Weinert,T.A. (1989) Checkpoints: controls that ensure the order of cell cycle events. *Science*, **246**, 629–634.

Kaiser,P., Sia,R.A.L., Bardes,E.G.S., Lew,D.J. and Reed,S.I. (1998) Cdc34 and the F-box protein Met30 are required for degradation of the Cdk-inhibitory kinase Swe1. *Genes Dev.*, **12**, 2587–2597.

King,R.W., Deshaies,R.J., Peters,J.M. and Kirschner,M.W. (1996) How proteolysis drives the cell cycle. *Science*, **274**, 1652–1659.

Lew,D.J. and Kornbluth,S. (1996) Regulatory roles of cyclin dependent kinase phosphorylation in cell cycle control. *Curr. Opin. Cell Biol*., **8**, 795–804.

Lew,D.J. and Reed,S.I. (1993) Morphogenesis in the yeast cell cycle: regulation by Cdc28 and cyclins. *J. Cell Biol*., **120**, 1305–1320.

Lew,D.J. and Reed,S.I. (1995) A cell cycle checkpoint monitors cell morphogenesis in budding yeast. *J. Cell Biol*., **129**, 739–749.

Lew,D.J., Weinert,T. and Pringle,J.R. (1997) Cell cycle control in *Saccharomyces cerevisiae*. In Pringle,J.R., Broach,J. and Jones,E. (eds), *The Molecular and Cellular Biology of the Yeast Saccharomyces*. Cold Spring Harbor Laboratory Press, Cold Spring Harbor, NY, pp. 607–695.

Lim,H.H., Goh,P.-Y. and Surana,U. (1996) Spindle pole body separation in *Saccharomyces cerevisiae* requires dephosphorylation of the tyrosine 19 residue of Cdc28. *Mol. Cell. Biol*., **16**, 6385–6397.

Liu,H. and Bretscher,A. (1989) Disruption of the single tropomyosin gene in yeast results in the disappearance of actin cables from the cytoskeleton. *Cell*, **57**, 233–242.

Liu,H. and Bretscher,A. (1992) Characterization of *TPM1* disrupted yeast cells indicates an involvement of tropomyosin in directed vesicular transport. *J. Cell Biol*., **118**, 285–299.

Lundgren,K., Walworth,N., Booher,R., Dembski,M., Kirschner,M. and Beach,D. (1991) mik1 and wee1 cooperate in the inhibitory tyrosine phosphorylation of cdc2. *Cell*, **64**, 1111–1122.

Ma,X.-J., Lu,Q. and Grunstein,M. (1996) A search for proteins that interact genetically with histone H3 and H4 amino termini uncovers novel regulators of the Swe1 kinase in *Saccharomyces cerevisiae*. *Genes Dev.*, **10**, 1327–1340.

McGowan,C.H. and Russell,P. (1995) Cell cycle regulation of human WEE1. *EMBO J*., **14**, 2166–2175.

McMillan,J.N., Sia,R.A.L. and Lew,D.J. (1998) A morphogenesis checkpoint monitors the actin cytoskeleton in yeast. *J. Cell Biol*., **142**, 1487–1499.

Morgan,D.O. (1995) Principles of CDK regulation. *Nature*, **374**, 131–134.

Murray,A.W. (1992) Creative blocks: cell-cycle checkpoints and feedback controls. *Nature*, **359**, 599–604.

Nugroho,T.T. and Mendenhall,M.D. (1994) An inhibitor of yeast cyclin-dependent protein kinase plays an important role in ensuring the genomic integrity of daughter cells. *Mol. Cell. Biol*., **14**, 3320–3328.

Nurse,P. (1990) Universal control mechanism regulating onset of M-phase. *Nature*, **344**, 503–508.

O'Connell,M.J., Raleigh,J.M., Verkade,H.M. and Nurse,P. (1997) Chk1 is a wee1 kinase in the G2 DNA damage checkpoint inhibiting cdc2 by Y15 phosphorylation. *EMBO J*., **16**, 545–554.

Peng,C.-Y., Graves,P.R., Thoma,R.S., Wu,Z., Shaw,A.S. and Piwnica-Worms,H. (1997) Mitotic and G_2 checkpoint control: regulation of 14-3-3 protein binding by phosphorylation of Cdc25C on serine-216. *Science*, **277**, 1501–1505.

Pringle,J.R., Adams,A.E.M., Drubin,D.G. and Haarer,B.K. (1991) Immunofluorescence methods for yeast. *Methods Enzymol*., **194**, 565–602.

Rhind,N. and Russell,P. (1998) Tyrosine phosphorylation of cdc2 is required for the replication checkpoint in *Schizosaccharomyces pombe*. *Mol. Cell. Biol*., **18**, 3782–3787.

Rhind,N., Furnari,B. and Russell,P. (1997) Cdc2 tyrosine phosphorylation is required for the DNA damage checkpoint in fission yeast. *Genes Dev.*, **11**, 504–511.

Russell,P., Moreno,S. and Reed,S.I. (1989) Conservation of mitotic controls in fission and budding yeast. *Cell*, **57**, 295–303.

Sanchez,Y., Wong,C., Thoma,R.S., Richman,R., Wu,Z., Piwnica-Worms,H. and Elledge,S.J. (1997) Conservation of the Chk1 checkpoint pathway in mammals: linkage of DNA damage to Cdk regulation through Cdc25. *Science*, **277**, 1497–1501.

Schwob,E., Bohm,T., Mendenhall,M.D. and Nasmyth,K. (1994) The B-type cyclin kinase inhibitor $p40^{SIC1}$ controls the G_1 to S transition in *S.cerevisiae*. *Cell*, **79**, 233–244.

Sia,R.A.L., Herald,H.A. and Lew,D.J. (1996) Cdc28 tyrosine phosphorylation and the morphogenesis checkpoint in budding yeast. *Mol. Biol. Cell*, **7**, 1657–1666.

Skowyra,D., Craig,K.L., Tyers,M., Elledge,S.J. and Harper,J.W. (1997) F-box proteins are receptors that recruit phosphorylated substrates to the SCF ubiquitin-ligase complex. *Cell*, **91**, 209–219.

Sloat,B.F., Adams,A.E.M. and Pringle,J.R. (1981) Roles of the *CDC24* gene product in cellular morphogenesis during the *Saccharomyces cerevisiae* cell cycle. *J. Cell Biol*., **89**, 395–405.

Sorger,P.K. and Murray,A.W. (1992) S-phase feedback control in budding yeast independent of tyrosine phosphorylation of $p34^{CDC28}$. *Nature*, **355**, 365–368.

Stueland,C.S., Lew,D.J., Cismowski,M.J. and Reed,S.I. (1993) Full activation of $p34^{CDC28}$ histone H1 kinase activity is unable to promote entry into mitosis in checkpoint-arrested cells of the yeast *Saccharomyces cerevisiae*. *Mol. Cell. Biol*., **13**, 3744–3755.

Tang,Z., Coleman,T.R. and Dunphy,W.G. (1993) Two distinct mechanisms for negative regulation of the Wee1 protein kinase. *EMBO J*., **12**, 3427–3436.

Received August 24, 1998; revised and accepted September 17, 1998